Plus Shaped Single Grating based Optical Fiber Structure for Water Sensing Application

Lokendra Singh (kashyap00000@gmail.com)
PARK COLLEGE OF ENGINEERING AND TECHNOLOGY https://orcid.org/0000-0003-3751-5975
NiteshKumar Agarwal
Indian Institute of Space Science and Technology
Chinmoy Saha
Indian Institute of Space Science and Technology
Prakash Pareek
Vishnu Institute of Technology

Research Article

Keywords: Fiber grating sensors, plua ahaped grating, transverse magnetic polarization, finite difference time domain (FDTD) method

Posted Date: May 6th, 2021

DOI: https://doi.org/10.21203/rs.3.rs-475600/v1

Abstract

Fiber grating sensors demonstrate great potential especially for the refractive index based sensing. However, a meticulous effort is still required to improve the sensitivity of fiber grating sensors towards water sensing. In this work, for the first time we have numerically investigated a plus shaped single grating within the core of optical fiber for water sensing applicaions. The primary objective of incoroporating the plus shaped grating within the core is to increase the sensitivity in comparison to existing grating sensors while increasing the analytes quantity. The testing of designed grating sensor model is done within the refractive index range from 1.33 to 1.39 with a remarkable wavelength shift of 65 nm. The analysis of proposed model of grating sensor is accomplished by using finite difference time domain (FDTD) method under the contour of perfect matched layer (PML) as boundary conditions at the interface of core and grating. The attained results depicts the significant sensitivity of the proposed fiber grating sensor for water sample sensing.

I. Introduction

THE concentration of water pollutants is extensively studied for various applications in the area of oceanography, clinical testing, food testing, and quality monitoring of water resources [1–3]. In traditional techniques, water pollutant detection techniques, the detection of presence of ion concentration in water was done on the basis of conductivity which is highly sensitivity to electromagnetic interference. As a result such techniques were not able to fulfill the demand of high precision and sensitivity which are desirable from competent water sample sensor [4]. The optical fiber based sensors are of great interest because of their wide application domains, immune to electromagnetic interference, easiest miniaturization and remote control [5] [6]. The expectation of new technological solutions is proportionally increasing with the growing demand of optical fiber based sensors and biosensors. The optical fibers were included in sensing applications to increase the sensitivity of sensor systmes [7]. Various optical fiber based models were utilized for the salinity sensing, that increases due to the presence of ions in water samples. Some notable attempts are fiber based interferometers [8–12]. tapered fibers [13, 14], photonic crystal fibers (PCF's) [15, 16], surface plasmon resonance (SPR) sensors [17, 18], microfiber [4, 19] and fiber grating sensors [20–23]. However, the interferometeric probes were less sensitive when immersed into the targeted samples. The tapered fiber sensor structures sustains higher sensitivity with precise calibration. PCF and SPR sensors exhibit higher sensitivity with higher costs and complicated fabrication procedures. The microfiber based sensors also exhibits higher sensitivity for external environment with precise adjustment of loop diameter to attain high reproducibility. Concurrently, the optical fiber grating have been extensively used for the numerous applications such as mode converters [24], wavelength selective devices [25], dispersion compensators [26], pulse compressors [27], and in sensing applications [28–32]. The fiber grating is designed by periodically modulating the core refractive index of optical fiber structure. On the basis of grating periods, the grating structures were classified into two categories: first, where the grating period is less than one micron and termed as Fiber Bragg Gratings (FBG) [33]. In another kind, the gratings period of hundreds of

microns is used and termed as long period grating (LPG) structures [34]. In FBG's, the fundamental mode of core gets coupled with its counterpropagating mode and optical signal not penetrates into cladding due to which the detection of external refractive index (RI) becomes impossible. Whereas, LPG in turn makes the coupling of fundamental core mode with cladding modes feasible that results into set of resonances in the transmission spectrum [28]. Therefore, the LPG's based sensors have been used for RI sensing [35], chemical sensing [36], and monitoring of variation in thin overlay films with high accuracy [37]. Moreover, these sensors receives attraction in biological sensing applications such as bacteria [38, 39], viruses [40], proteins [41], and nucleic acids [42]. Therefore, the overwhelming development of fiber grating based sensors leads to the development of different kind and geometry of gratings to achieve better sensitivity and accuracy. For instance, a V-shaped LPG based bending vector sensor has been proposed with effective dip in wavelength shift and higher sensitivity [30]. In an another approach, a D-shaped FBG based RI sensor has been proposed by side polishing the core layer after cleaving the half clad [31]. The main motivation behind the creation of different strucutres of grating is to improve the field distribution and to attain effective modulation that can produce better and precise results for RI sensing.

Therefore, in this work, for the first time we have numerically design and examined a plus shaped grating in optical fiber structure for the monitoring of ionic pollutants in water samples. Several studies have been reported for the RI based detection of ionic pollutants in water samples. For instance, a microfiber based Sagnac loop has been used for the detection of presence of chloride ions in water samples [4]. In another work, a corrugated fiber grating has been used for the detection of Lead ions in water samples. The RI of water samples containing ionic pollutants is ranges from 1.33–1.39 [43]. Therefore, in this work, we have analyzed the proposed sensor geometry under the RI ranges from 1.33 to 1.39, and as a result the wavelength shift of 65 nm was achieved while considering the perfect matched layers (PML) as boundary conditions at the interface of grating and core. The inclusion of plus shaped grating also increases the contact surface of sensor structure with analytes, that results into higher sensitivity. The analysis of designed structure of sensor model was carried out by using fininte difference time domain (FDTD) method. The paper comprises five sections: the introductory part of the work paper is covered in Section I. Section II and III, present the designing of proposed sensor model and corresponding results, respectively. A comparative analysis of proposed model is discussed in Section IV. The conclusion and future aspects of the work is discussed in Section V.

Ii. Designing Of Plus Shaped Single Grating

The design of plus shaped single grating structure in the core was implemented by analyszing the one single vertical slot of grating as presented in Fig. 1. The vertical single slot grating was modelled under the contour of perfect matched layer (PML) as boundary conditions at all the interfaces. The modelling of single vertical slot grating based sensor model was done in 12 μm long single mode optical fiber structure. A grating of 1 μm was created at the center of fiber structure. Moreover, in the model an appropriate ratio of core and cladwas considered in such a way that analysis was carried out at the core lateral width of 1.125 μm. The RI of substrate was optimized equal to the RI of cladding of optical fiber. The propagation of optical signal through the core is guided by obeying the well established coupled

mode theory [44, 45]. The variation of effective refractive index in the fiber core due to the presence of grating can be modelled as [44];

$$\frac{n(z)}{n_0} = 1 + \sigma(h_0 z) + \ 2\text{þ}(h_0 z)\cos[2h_0 z + \emptyset(h_0 z)] \qquad (1)$$

where, h_0 is the wavenumber at resonant wavelength on which design is modelled, n_0 is the the refractive index of unmodified core, σ, þ and Φ are the slowly varying functions of factor $h_0 z$. For the gratings, if we consider factor þ to be very smaller than 1 i.e. þ≪1, then the detuning factor can be describe mathematically as;

$$\Delta = \frac{\omega - \omega_0}{\omega_0} \qquad (2)$$

Where, ω is the frequency, and the sum of electric fields of forward and backward propagating modes is written as;

$$E(\varsigma) = a_+(\varsigma)exp\left\{i\left[\varsigma + \frac{1}{2}\emptyset(\varsigma)\right]\right\} + a_-(\varsigma)exp\left\{-i\left[\varsigma + \frac{1}{2}\emptyset(\varsigma)\right]\right\} \qquad (3)$$

The coupled mode theory can be used for deriving the fields for forward and backward propagating modes. This theory is applicable for the monochromatic frequency or continuous wave (CW) source especially for linear propagation, whereas, for the pulsed input signal, it can be validated by separately considering each spectral component over the spectrum of incident pulse signal [46]. The optimized parameters of theoretical analysis can be carried forward for the fabrication of sensor model. Whereas, in first appearance, the design of plus shaped cavity seems to be difficult in terms of fabrication, but can be easily done by using following approach: A focused ion beam (FIB) technique can be taken into consideration to fabricate the plus shaped cavity. By employing the sputtering technique to take out the fiber molecules with accelerated ions, holes or cavities in micro-scale. The micro-trenches developed by FIB technique on micro and taper fibers have proven to be feasible [47, 48]. In larger dimension fibers, FIB has been also used to mill side-accessed holes in air silica structured fibers [49]. The FIB-fabricated grating structures have shown potential for the application of temperature and refractive index (RI) sensors [50]. The fundamental element for creating the plus shaped cavity in fiber with aspect ratio is that the cavity should be deep enough to interact with the propagating fields and its width should be 1 micron. The investigation of FIB process on silicon has been already proven to successful [51]. However, in contrast, it is still challenging to attain a high aspect ratio cavity or hole in bulk silicon substrate [52]. The aspect ratio can be increased for gas assisted FIB technique and also feasible for optical fibers [52]. To, fabricate the desired plus shaped cavity, initially the plastic jacket of fiber can be manually removed. Then, fiber will be kept under scanning electron microscope while covering it with the conducting tape. Thereafter, the pattern of plus shaped cavity can be drawn over the conducting tape. Initially, the etching can be done with the depth ratio of 10 microns to maintain the fiber strength. The etching process can be continued till the desired cavity attained. The fabrication of desired plus shaped cavity under FIB can be

done by using Gallium ion dual beam accelerating at 30 keV. The drawn can be set to 50 nA with beam spot size of 300 nm [53]. The RI distribution of the model of single vertical slot grating based sensor model is presented in Fig. 2. From the RI distribution profile, one can easily observe the presence of vertical slot filled with RI in the tune of 1.33 similar to real water samples. Thereafter, the results of single vertical grating has been taken into consideration and plus shaped grating based sensor is modelled as shown in Fig. 3. The plus shaped grating was modelled by including the lateral slot of length and width of 1.6 μm and 1 μm, respectively, with the single vertical slot having width of 1 μm in the propagating direction.

Iii. Results And Discussion

The theoretical analysis and formulation was followed stepwise to achieve the precise results. The investigation of plus shaped grating based sensor model was followed by the analysis of models of linear fiber core and single vertical slot grating. Initially, fiber structure was studied in detail to optimize the numerical parameters such as meshing, line width of source, boundary conditions, polarization, operating wavelength and power of the input source. The analysis of all the designed models was done under the similar parameters. The meshing of 0.25 × 0.25 micron was taken into consideration with transverse magnetic (TM) polarization with PML as boundary conditions at all the interfaces of grating and core. The propagation of optical signal within the optical fiber core was carried out at the wavelength of 1.55 μm with the confined linewidth of 0.39 μm and the input power of 1 W/μm. For the clear understanding of all three structures which are considered in this work, (linear core, single vertical slot grating and plus shaped grating) their detail simulation was carried out and corresponding results provided separately in the respective sections. The analysis of water samples was done in the RI range of 1.33 to 1.39. Under the tested RI range of water samples, almost all the ionic pollutants are covered which are degrading the water quality.

A. Linear fiber core structure

The analysis of linear fiber core structure was done in terms of signal transmission, distribution of mode profile, phase distribution in direetion of propagation and power confinement as shwon in Fig. 4. The transmission of optical signal through the core is presented in Fig. 4 (a), from where it can be observed that at operating wavelength the maximum power is confined within the core. The distribution of propagating mode profile also shown in Fig. 4 (b), from where it was conceived that the mode distribution is uniform throughout the core. The mode distribution profile also depicts the confinement of optical power in the center of core along the propagation axis. The phase distribution of the propagating field is exactly matched with the mode distribution profile of field, as provided in Fig. 4(c). The graphical representation of optical field confinement within the core of fiber is presented in Fig. 4 (d). It can be easily concluded from this figure that maximum power is confined within the center part of core along the axis of propagation, which is about 0.9 a.u.

B. Single vertical slot grating

The analysis of single vertical slot grating structure was followed by the results of linear fiber core model. A 1-μm wide vertical grating was created at the center of linear fiber core. Thereafter, for analyzing the water samples, RI of vertical grating was set to 1.33 which is equivalent to the water RI.

The performance of designed structure was gauged in terms of transmission of optical signal, mode and phase distribution and power confinement in core region as revealed in Fig. 5. The propagation of optical fields through the single vertical slot grating incorporated fiber is presented in Fig. 5 (a). It can be infer from the figure that a part of power was absorbed at the created grating slot and hence power at output is low in comparison of linear optical fiber core structure which was discussed in previous section. Instead of absorption, a part of power is also decaying into substrate region which is considered as outer environment in proposed work as shown in Fig. 5 (b). The power leaked into external environment is not going to recombine with the field propagating inside the core and grating structures. The phase distribution of the fields can be seen from Fig. 5 (c). This figure gives a clear understanding of the nature of variation in phase of signal propagating through the created grating. The loss in power at output can be comprehend from Fig. 5 (d), which clearly reveals that the power at the output port of designed sensor structure is low in comparison of linear optical fiber structure (as depicted in Fig. 4(d).

Afterwards, the analysis of designed sensor structure was done by varying the width of slot from 0.5 nm to 1 μm, and results were obtained in terms of output intensity with respect to slot width as shown in Fig. 6. The analysis was carried out to examine the slot width for the modelling of plus shaped cavity sensor model. The output results illustrates that on narrowing the slot width below 1 μm, the output power profile is also degrading. The power at output port for the slot width less than 100 nm is presented in inset of Fig. 6. For the slot width less than 100 nm, the power at output port almost degraded by 25 %. This loss in power at output port on narrowing down the width of grating slot below 100 nm is because of the decaying of field in outer environment with poor confinement in core. Therefore, it can be concluded that for proposed geometry of sensor higher sensitivity can be attained at the slot widths higher than 100 nm. The results indicates that the output power profile was sharply increases for the slot width greater than 400 nm and goes till 850 nm. Afterwards, the output power linearly increased for the slot width higher than 850 nm and almost get saturated after 1 μm. The maximum output power was attained at the slot width of 1 μm, which has been used to examine the sensing ability of plus shaped cavity. The pictorial representation of power confinement in the core at the slot width of 10 nm is presented in Fig. 7, tbat is around 75 % of the input power.

C. Plus shaped grating structure

The results of single vertical slot grating structure as discussed in previous section were taken into consideration to analyze plus shaped grating structure. The plus shaped grating model was introduced by including a lateral slot of length and width of 1.6 μm and 1 μm, respectively, as shown in Fig. 3. Inspection of designed plus shaped grating structure was done by analyzing field propagation and confinement of optical field in the core as provided in Fig. 8. The optical field propagation presented in Fig. 8 (a) is plotted for the slot widths of 1 μm, which deduce that almost 25 % of power is excreted into

external environment. The graphical representation of optical power confinement within the core is depicted in Fig. 8 (b). From where the degree of optical power confinement within the core is studied under variation of the slot width from 0.5 nm to 1 μm. This result illustrate that maximum power is confined within the core when slot width set equals to 1 μm. Then, structure was investigated further under deviation of slot widths with power at output port, and obtained results are presented in Fig. 9.

The trend shown in Fig. 9 states that on increasing the slot widths to higher values the transmitted power at output port is also increasing proportionally. However, similar to single slot vertical grating there was no such remarkable variation in output power for narrower widths of plus grating slots ranging from 0.5 to 100 nm. The output power profile for narrower slot widths is also shown in inset of Fig. 9. The maximum output power was obtained for the slot width of 1 μm while keeping fixed length. Thereafter, the sensing ability of plus shaped grating model was gauged by varying the RI from 1.33 to 1.39. The analysis of proposed plus shaped grating was done in presence of RI of water ranging from 1.33 to 1.39, which covers all the ionic pollutants. The presence of ionic pollutants in water leads to the increase in its refractive index, which is vulnerable for aquatic lives. Also, it degrades the quality of drinking water that becomes a key issue in developing countries. The analysis of sensor was initiated at the wavelength of 1550 nm for the RI of 1.33. The shift in wavelength with respect to RI is presetnd in Fig. 10. From the results, it can be comprehended that on increase in RI leads to red shift in waveglength and total shift was about 65 nm for the tested range of RI. The attained results also states that the sensitivity of designed plus shaped grating structure is 1083 nm/RIU with the autocorrelation function of 99.69 %.

Iv. Comparative Analysis

A co mparative study of proposed work with relevant reported water sensing models is presented in Table 1. This study is done in terms of obtained autocorrelation coefficient and sensitivity. A FBG based sensor was developed for the detection of water level [46]. The development of sensor structure was done by using converntional FBG, whereas, in our work, we have introduced a novel plus shaped grating to sense the water samples. In an another work, a normal optical fiber based sensor structure was implemented for water quality monitoring with fine autocorrelation coefficient but there was no discussion about the sensitivity of sensor [47]. A corrugated fiber grating structure was developed for the detection of lead ions in water samples. Although, the work was fruitful but the autocorrelation coefficient and sensitivity of the sensor was not reported [48]. A portable optical fiber structure has been used for the detection of E-Coli in water samples. The sensor implementation was done with the autocorrelation function of 0.95 [54]. An optical fiber based Mach-Zehnder interferometer (MZI) has been reported for the monitoring of water level. The reported sensor is capable of monitoring the water level with the autocorrelation function and sensitivity of 0.99 and 1868.42 pm/nm/RIU, respectively [55]. In an another work, a D-shaped FBG was deployed for the detection of liquid samples including water [38]. The work highlighted a unique novel D-shaped FBG sensor structure, but autocorrelation coefficient and sensitivity of sensor was not addressed. A linear optical fiber cable based sensor structure was also reported for the detection of water level. The sensor structure was capable of sensing the detecting the level with autocorrelation function and sensitivity of 0.9616 and 329.22 nm/RIU, respectively [56]. In present work, a

novel plus shaped grating structure is precisely designed numerically and investigated for the monitoring of water samples containing ionic pollutants. A wide range of RI (1.33–1.39) is considered in present work that includes numerous ionic pollutants contaminating the drinking water. For the proposed sensor model, the attained autocorrelation coefficient and sensitivity are 0.9969 and 1083 nm/RIU, respectively.

Table 1
A comparative analysis of proposed work with reported water sensing sensor models.

Sensor structure	Used analytes	Autocorrelation coefficient (R^2)	Sensitivity	Ref.
FBG	Water level	0.9986	0.00639 nm/cm	[57]
Optical fiber sensor	Water quality	0.958	n.r.*	[58]
Portable optical fiber	E-Coli in waste water	0.95	n.r.*	[54]
Fiber based MZI	Water level	0.99	1868.42 (pm/mm)/RIU	[59]
Corrugated Fiber grating	Lead ion detection in water	n.r.*	n.r.*	[60]
Linear optical fiber	Water level	0.9616	329.22 pm/nm/RIU	[56]
D-shpaed FBG	Liquid samples including water	n.r.*	n.r.*	[31]
Plus shaped grating	Water samples	0.9969	1083 nm/RIU	This work

n.r.*- not reported

V. Conclusion

In this work, a novel design of a plus shaped grating structure has been proposed along with its theoretical analysis. The sensing capability of designed structure was judged by testing the range of RI from 1.33–1.39 which covers almost all the ionic pollutants responsible for contaminating the water resources. The detailed analysis of designed grating structure was carried out stepwise. Initially, linear fiber core structure was discussed and its charateristics were determined in terms of transmission of optical signals, mode and phase distribution profile and confinement of optical power within the core of fiber structure. Secondly, single vertical slot grating was introduced and relevant charcteristics were determined. Finally lateral grating slot was incorporated in the structure to form a plus shaped grating which is studied for its performance as water sample sensor. Simulation of the proposed structure was implemented by using finite difference time domain (FDTD) technique based software tool at 1550 nm. Wavelength shifting on introduction of external environment in plus shaped grating structure indicates

that the designed sensor structure is having high sensitivity towards water samples which is about 1083 nm/RIU with the autocorrelation function coefficient of 99. 69 %. The possible reason behing this high sensitivity can be explained as follows: 1) contact surface of sensor strucuture with analytes increases due to incorporation of plus shaped graing, 2) Another salient advantage of this structure is non requirement of creating too many gratings due to enhancement of analyte content within single plus shaped grating structure. Therefore, the innovative structure of plus shaped grating could be a point of attraction for the development of optical fiber based biosensors especially for the monitoring of water samples and biological molecules.

Vi. Declarations

Conflict of Interest

We all the authors declare that there is no conflict of interest.

Funding

There is no funding for the proposed work.

Author’s contribution

The idea was given by first author and he also drafted the file. The result analysis was done by second and third author. The fourth author updated the draft file of manuscript.

Availibility of data and material

There is no supportive data and material available with the manuscript.

Code availability

There is no code available with the manuscript.

Ethics approval

There was no such need of ethics approval to comprise the proposed work.

Consent to participate and publication

We all the authors take all the responbiliteis of publication of manuscript.

Vii. References

1. Zhang X, Zhao T, Yuan B, Zhang S, "Optical Salinity Sensor System Based on Fiber-Optic Array," *Sensors Journal, IEEE*, vol. 9, pp. 1148–1153, 10/01 2009

2. Hangzhou Y, Qiao X-G, Lim K-S, Harun SW, Chong W-Y, Islam MR et al, "Optical Fiber Sensing of Salinity and Liquid Level," *Photonics Technology Letters, IEEE*, vol. 26, pp. 1742–1745, 09/01 2014
3. Xie N, Zhang H, Liu B, Liu H, Liu T, Wang C (2018) In-Line Microfiber-Assisted Mach–Zehnder Interferometer for Microfluidic Highly Sensitive Measurement of Salinity. IEEE Sens J 18:8767–8772
4. Zu L, Zhang H, Miao Y, Li B, Yao J, "Microfiber coupler with a Sagnac loop for water pollution detection," *Applied Optics*, vol. 58, pp. 5859–5864, 2019/07/20 2019
5. Culshaw B (2004) "Optical fiber sensor technologies: opportunities and-perhaps-pitfalls". J Lightwave Technol 22:39–50
6. Lee B (2003) "Review of the present status of optical fiber sensors". Opt Fiber Technol 9:57–79 2003/04/01/
7. Hunt HK, Armani AM, "Label-free biological and chemical sensors," *Nanoscale*, vol. 2, pp. 1544–1559, 2010
8. Shi L, Xu Y, Tan W, Chen X (2007) "Simulation of Optical Microfiber Loop Resonators for Ambient Refractive Index Sensing. Sensors 7:689–696
9. Zhao P, Shi L, Liu Y, Wang Z, Zhang X, "Compact in-line optical notch filter based on an asymmetric microfiber coupler" *Appl Opt*, vol. 52, pp. 8834–9, Dec 20 2013
10. Zhu S, Liu Y, Shi L, Xu X, Zhang X, "Extinction ratio and resonant wavelength tuning using three dimensions of silica microresonators" *Photonics Research*, vol. 4, pp. 191–196, 2016/10/01 2016
11. Meng Q, Dong X, Ni K, Li Y, Xu B, Chen Z (2014) Optical Fiber Laser Salinity Sensor Based on Multimode Interference Effect. IEEE Sens J 14:1813–1816
12. Jaddoa MF, Jasim AA, Razak MZA, Harun SW, Ahmad H, "Highly responsive NaCl detector based on inline microfiber Mach–Zehnder interferometer" *Sensors and Actuators A: Physical*, vol. 237, pp. 56–61, 2016/01/01/ 2016
13. Rahman HA, Harun SW, Yasin M, Phang SW, Damanhuri SSA, Arof H, *et al.*, "Tapered plastic multimode fiber sensor for salinity detection," *Sensors and Actuators A: Physical*, vol. 171, pp. 219–222, 2011/11/01/ 2011
14. Liao Y, Wang J, Yang H, Wang X, Wang S (2015) Salinity sensing based on microfiber knot resonator. Sensors Actuators A: Physical 233:22–25 2015/09/01/
15. Kwon M-S, Cho Y-B, Shin S-Y (2006) Experimental demonstration of a long-period grating based on the sampling theorem. Applied Physics Letters - APPL PHYS LETT 88:05/21
16. Wu C, Tse M-LV, Liu Z, Guan B-O, Zhang AP, Lu C, *et al.*, "In-line microfluidic integration of photonic crystal fibres as a highly sensitive refractometer," *Analyst*, vol. 139, pp. 5422–5429, 2014
17. Gentleman DJ, Booksh KS, "Determining salinity using a multimode fiber optic surface plasmon resonance dip-probe," *Talanta*, vol. 68, pp. 504–515, 2006/01/15/ 2006
18. Díaz-Herrera N, Esteban O, Navarrete MC, Haitre ML, González-Cano A, "In situsalinity measurements in seawater with a fibre-optic probe" *Measurement Science and Technology*, vol. 17, pp. 2227–2232, 2006/07/13 2006

19. Wei F, Mallik A, Liu D, Wu Q, Peng G-D, Farrell G et al (2017) Magnetic field sensor based on a combination of a microfiber coupler covered with magnetic fluid and a Sagnac loop. Sci Rep 7:12/01
20. Men L, Lu P, Chen Q, "A multiplexed fiber Bragg grating sensor for simultaneous salinity and temperature measurement" *Journal of Applied Physics - J APPL PHYS*, vol. 103, 03/01 2008
21. Possetti GRC, Kamikawachi RC, Prevedello CL, Muller M, Fabris JL, "Salinity measurement in water environment with a long period grating based interferometer" *Measurement Science and Technology*, vol. 20, p. 034003, 2009/02/04 2009
22. Zhou W, Mandia DJ, Barry ST, Albert J, "Absolute near-infrared refractometry with a calibrated tilted fiber Bragg grating," *Opt Lett*, vol. 40, pp. 1713–6, Apr 15 2015
23. Yang F, Sukhishvili S, Du H, Tian F (2017) Marine salinity sensing using long-period fiber gratings enabled by stimuli-responsive polyelectrolyte multilayers. Sens Actuators B 253:745–751 2017/12/01/
24. Hill KO, Malo B, Vineberg K, Bilodeau F, Johnson DC, Skinner I, "Efficient mode conversion in telecommunication fibre using externally written gratings" *Electronics Letters*, vol. 26, pp. 1270–1272, 09/02 1990
25. Bilodeau F, Hill KO, Malo B, Johnson DC, Albert J, "High-return-loss narrowband all-fiber bandpass Bragg transmission filter," *Photonics Technology Letters, IEEE*, vol. 6, pp. 80–82, 02/01 1994
26. Ouellette F (Oct 1 1987) Dispersion cancellation using linearly chirped Bragg grating filters in optical waveguides. Opt Lett 12:847–849
27. Eggleton BJ, Krug PA, Poladian L, Ahmed KA, Liu HF, "Experimental demonstration of compression of dispersed optical pulses by reflection from self-chirped optical fiber Bragg gratings" *Opt Lett*, vol. 19, pp. 877–9, Jun 15 1994
28. Janczuk-Richter M, Dominik M, Koba M, Mikulic P, Bock WJ, Maćkowski S et al (2019) "Water-Induced Fused Silica Glass Surface Alterations Monitored Using Long-Period Fiber Gratings". J Lightwave Technol 37:4542–4548
29. Warren-Smith SC, Schartner EP, Nguyen LV, Otten DE, Yu Z, Lancaster DG et al (2019) "Stability of Grating-Based Optical Fiber Sensors at High Temperature". IEEE Sens J 19:2978–2983
30. Zhang Y, Zhang W, Yan T, Bie L, Zhang Y, Wang S et al (2018) "V-Shaped Long-Period Fiber Grating High-Sensitive Bending Vector Sensor". IEEE Photonics Technol Lett 30:1531–1534
31. Chen H-W, Tien C-L, Liu W-F, Lin S-W, *The Measurement of Liquid Refractive Index by D-shaped Fiber Bragg Grating*, 2007
32. Guo J, Yang C (2015) Highly Stabilized Phase-Shifted Fiber Bragg Grating Sensing System for Ultrasonic Detection. IEEE Photonics Technol Lett 27:848–851
33. Hill KO, Meltz G (1997) Fiber Bragg grating technology fundamentals and overview. J Lightwave Technol 15:1263–1276
34. Vengsarkar AM, Lemaire PJ, Judkins JB, Bhatia V, Erdogan T, Sipe JE (1996) Long-period fiber gratings as band-rejection filters. J Lightwave Technol 14:58–65

35. Xuewen S, Lin Z, Bennion I (2002) Sensitivity characteristics of long-period fiber gratings. J Lightwave Technol 20:255–266
36. Korposh S, Selyanchyn R, Yasukochi W, Lee S-W, James SW, Tatam RP, "Optical fibre long period grating with a nanoporous coating formed from silica nanoparticles for ammonia sensing in water," *Materials Chemistry and Physics*, vol. 133, pp. 784–792, 2012/04/16/ 2012
37. Śmietana M, Mikulic P, Bock WJ (2018) Nano-coated long-period gratings for detection of sub-nanometric changes in thin-film thickness. Sensors Actuators A: Physical 270:79–83 2018/02/01/
38. Brzozowska E, Koba M, Śmietana M, Górska S, Janik M, Gamian A et al (2016) "Label-free Gram-negative bacteria detection using bacteriophage-adhesin-coated long-period gratings". Biomedical optics express 7:829–840
39. Bandara AB, Zuo Z, Ramachandran S, Ritter A, Heflin JR, Inzana TJ, "Detection of methicillin-resistant staphylococci by biosensor assay consisting of nanoscale films on optical fiber long-period gratings," *Biosensors and Bioelectronics*, vol. 70, pp. 433–440, 2015/08/15/ 2015
40. Janczuk-Richter M, Dominik M, Roźniecka E, Koba M, Mikulic P, Bock WJ, *et al.*, "Long-period fiber grating sensor for detection of viruses," *Sensors and Actuators B: Chemical*, vol. 250, pp. 32–38, 2017/10/01/ 2017
41. Chiavaioli F, Biswas P, Trono C, Jana S, Bandyopadhyay S, Basumallick N et al, "Sol–Gel-Based Titania–Silica Thin Film Overlay for Long Period Fiber Grating-Based Biosensors" *Analytical Chemistry*, vol. 87, pp. 12024–12031, 2015/12/15 2015
42. Czarnecka KH, Dominik M, Janczuk-Richter M, Niedziółka-Jönsson J, Bock WJ, Śmietana M, "Specific detection of very low concentrations of DNA oligonucleotides with DNA-coated long-period grating biosensor," 2017, p. 1032313
43. Wang S, Zu L, Miao Y, Fei C, Zhang H, Li B et al, "Simultaneous measurement of the BOD concentration and temperature based on a tapered microfiber for water pollution monitoring" *Appl Opt*, vol. 59, pp. 7364–7370, Aug 20 2020
44. Sipe JE, Poladian L, de Sterke CM, "Propagation through nonuniform grating structures" *Journal of the Optical Society of America A*, vol. 11, pp. 1307–1320, 1994/04/01 1994
45. Mizrahi V, Sipe JE (1993) Optical properties of photosensitive fiber phase gratings. J Lightwave Technol 11:1513–1517
46. Agrawal GP, "Nonlinear Fiber Optics," in *Nonlinear Science at the Dawn of the 21st Century*, Berlin, Heidelberg, 2000, pp. 195–211
47. Kou J-L, Ding M, Feng J, Lu Y-Q, Xu F, Brambilla G, "Microfiber-Based Bragg Gratings for Sensing Applications: A Review," *Sensors*, vol. 12, pp. 8861–8876, 2012
48. Kou J-l, Qiu S-j, Xu F, Lu Y-q, "Demonstration of a compact temperature sensor based on first-order Bragg grating in a tapered fiber probe" *Optics Express*, vol. 19, pp. 18452–18457, 2011/09/12 2011
49. Martelli C, Olivero P, Canning J, Groothoff N, Gibson B, Huntington ST (07/01 2007) Micromachining structured optical fibers using focused ion beam milling. Opt Lett 32:1575–1577

50. Liu Y, Meng C, Zhang AP, Xiao Y, Yu H, Tong L, "Compact microfiber Bragg gratings with high-index contrast," *Optics Letters*, vol. 36, pp. 3115–3117, 2011/08/15 2011
51. Wico C, Hopman F, Ay W, Hu V, Gadgil L, Kuipers et al (05/16 2007) "Focused ion beam scan routine, dwell time and dose optimizations for submicrometre period planar photonic crystal components and stamps in silicon". NANOTECHNOLOGY Nanotechnology 18:195305–195311
52. Fu Y, Ngoi K, "Investigation of aspect ratio of hole drilling from micro to nanoscale via focused ion beam fine milling," 12/14 2004
53. Huang J, Alqahtani A, Viegas J, Dahlem M, *Fabrication of optical fiber gratings through focused ion beam techniques for sensing applications*, 2012
54. Yildirim N, Long F, Gu AZ, "Aptamer based E-coli detection in waste waters by portable optical biosensor system," in *2014 40th Annual Northeast Bioengineering Conference (NEBEC)*, 2014, pp. 1–3
55. Li L, Xie Z, Liu D (05/07 2012) All-fiber Mach-Zehnder interferometers for sensing applications. Optics express 20:11109–11120
56. Liang X, Liu Z, Wei H, Li Y, Jian S (2015) Detection of Liquid Level With an MI-Based Fiber Laser Sensor Using Few-Mode EMCF. IEEE Photonics Technol Lett 27:805–808
57. Vorathin E, Zohari MH, Ismail N, Loman M, Am A, Lim K-S et al, "FBG Water-Level Transducer based on PVC-Cantilever and Rubber-Diaphragm Structure" *IEEE Sensors Journal*, vol. PP, pp. 1–1, 05/13 2019
58. Omar A, Mat Jafri MZ (2008) "Development of Optical Fiber Sensor for Water Quality Measurement" vol 1017:05/01
59. Li L, Xia L, Xie Z, Liu D, "All-fiber Mach-Zehnder interferometers for sensing applications" *Optics Express*, vol. 20, pp. 11109–11120, 2012/05/07 2012
60. Chiniforooshan Y, Ma J, Bock W, Hao W, Wang Z, "Corrugated Fiber Grating for Detection of Lead Ions in Water" *Lightwave Technology, Journal of*, vol. 33, pp. 2549–2553, 06/15 2015

Figures

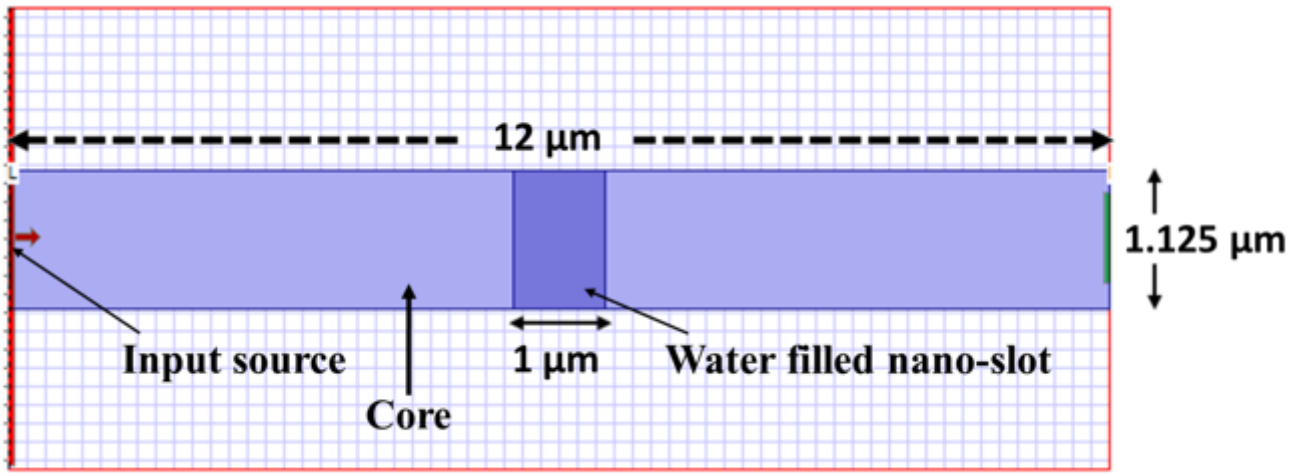

Figure 1

Layout design of single vertical grating based sensor model for water sensing.

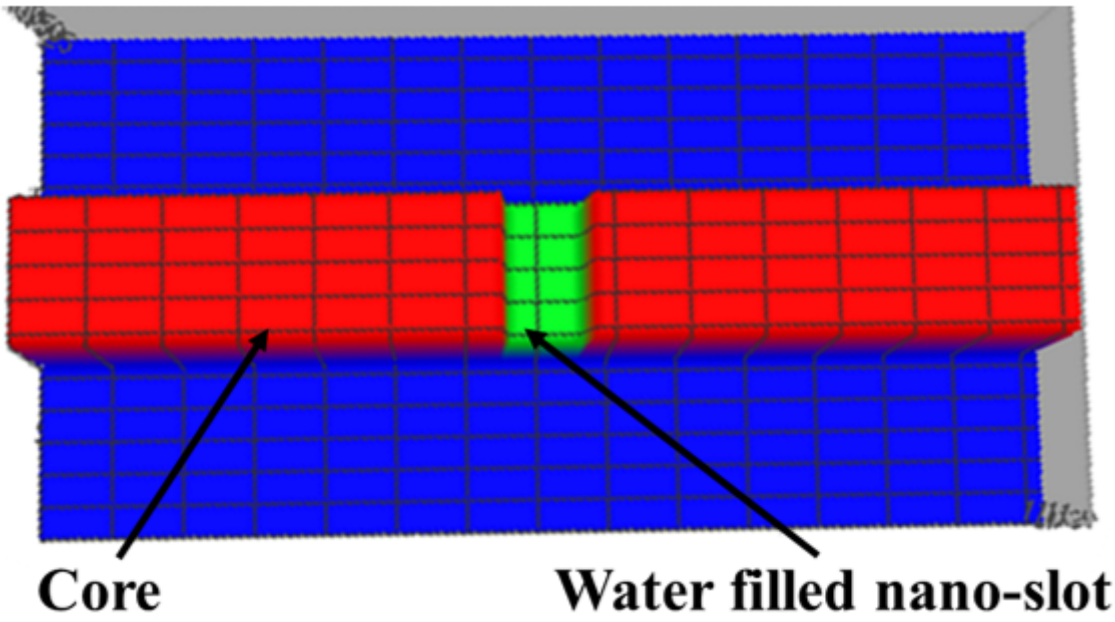

Figure 2

RI distribution of single vertical grating based sensor model for water sensing.

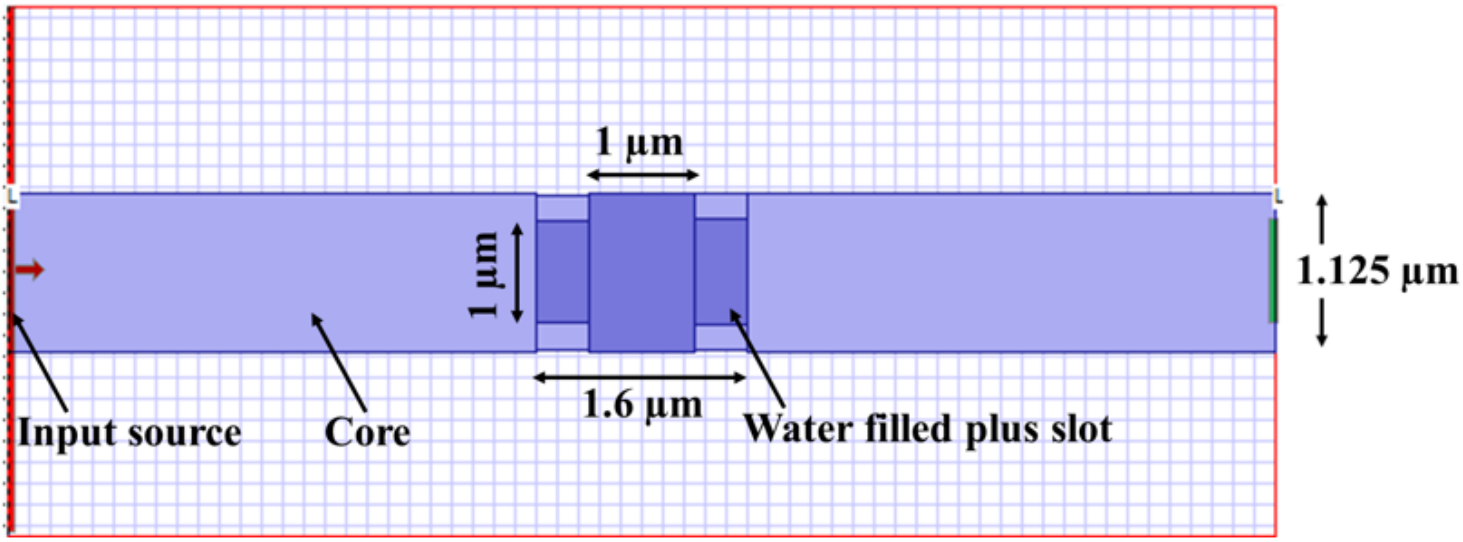

Figure 3

Layout design of single plus shaped grating based sensor model for water sensing.

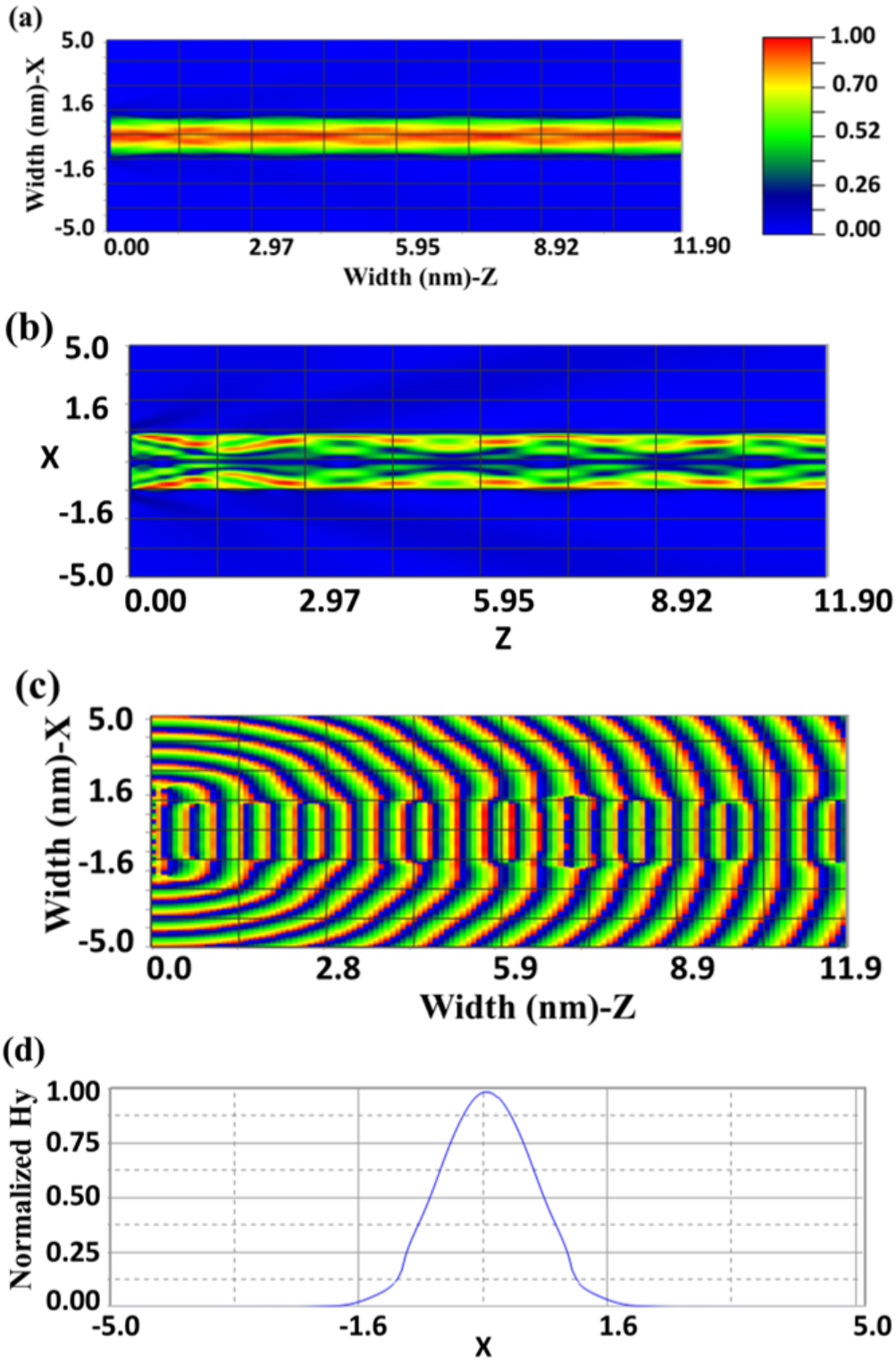

Figure 4

Analysis of linear fiber core structure: (a) optical transmission, (b) mode profile in direction of propagation, (c) phase distribution in direction of propagation, and (d) optical power confinement in core

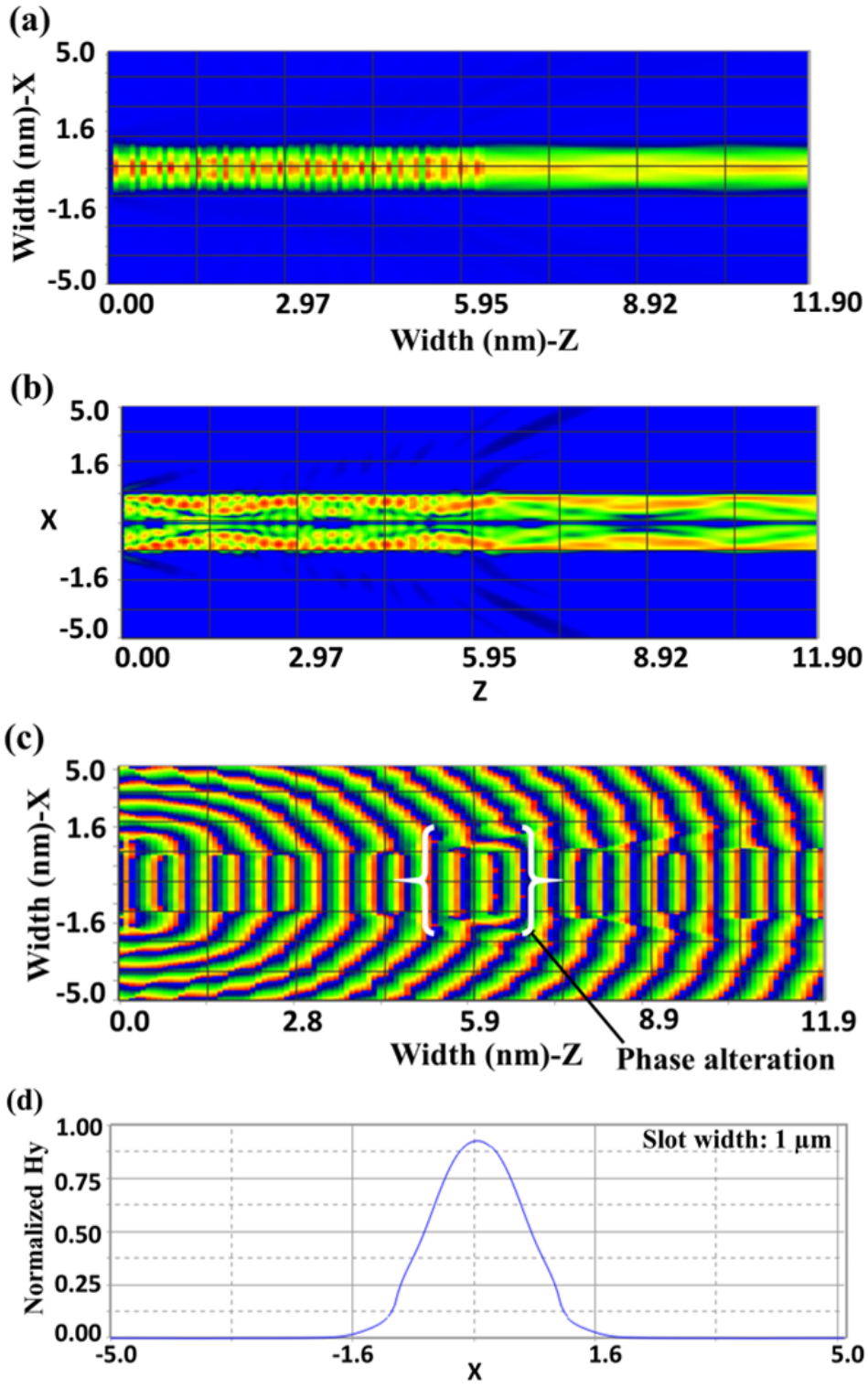

Figure 5

Analysis of single vertical slot grating structure: (a) Optical field transmission, (b) mode distribution in direction of propagation, (c) phase distribution in direction of propagation, and (d) power confinement in core.

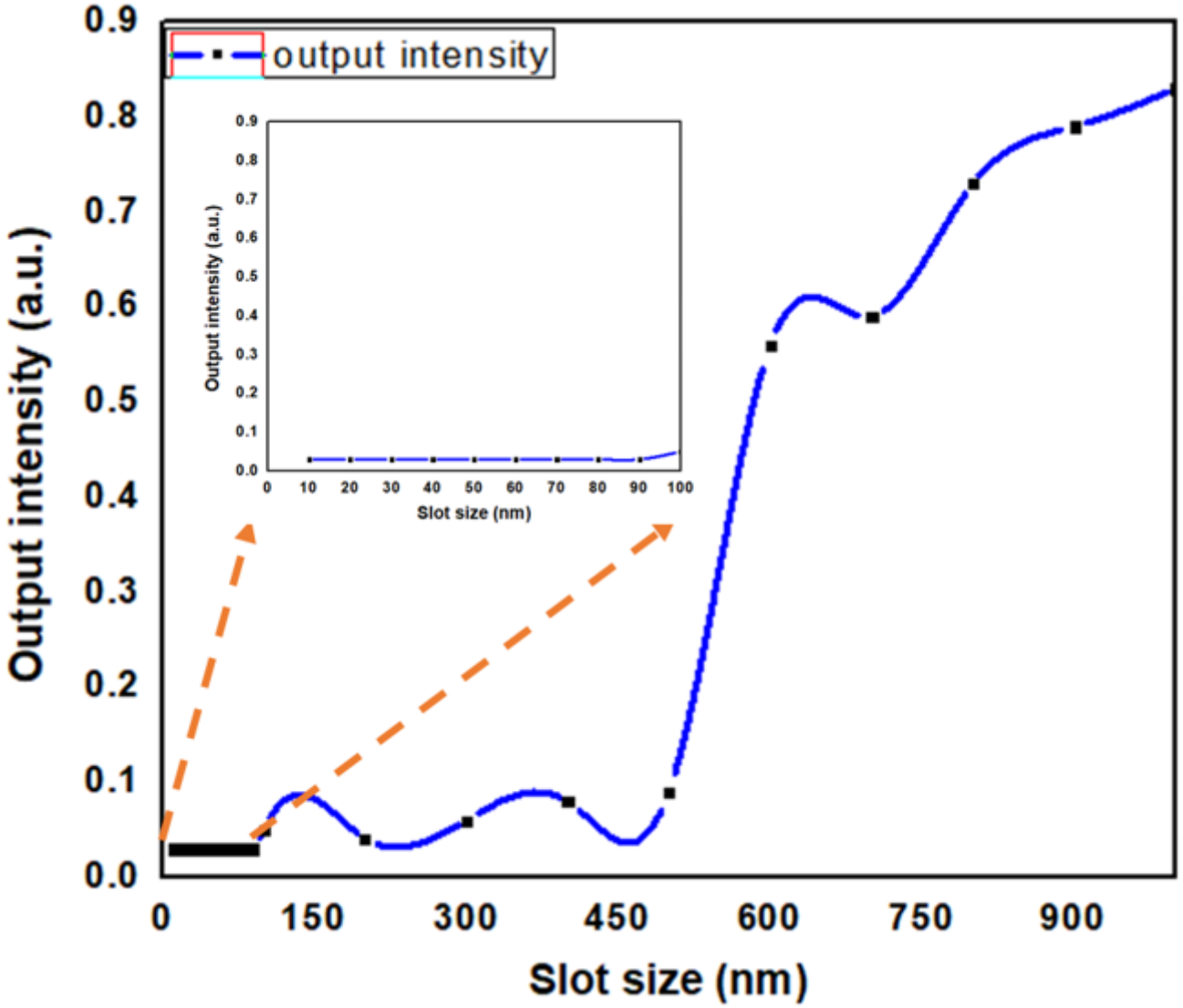

Figure 6

Plot of variation of width of single slot grating and respective output power transmission.

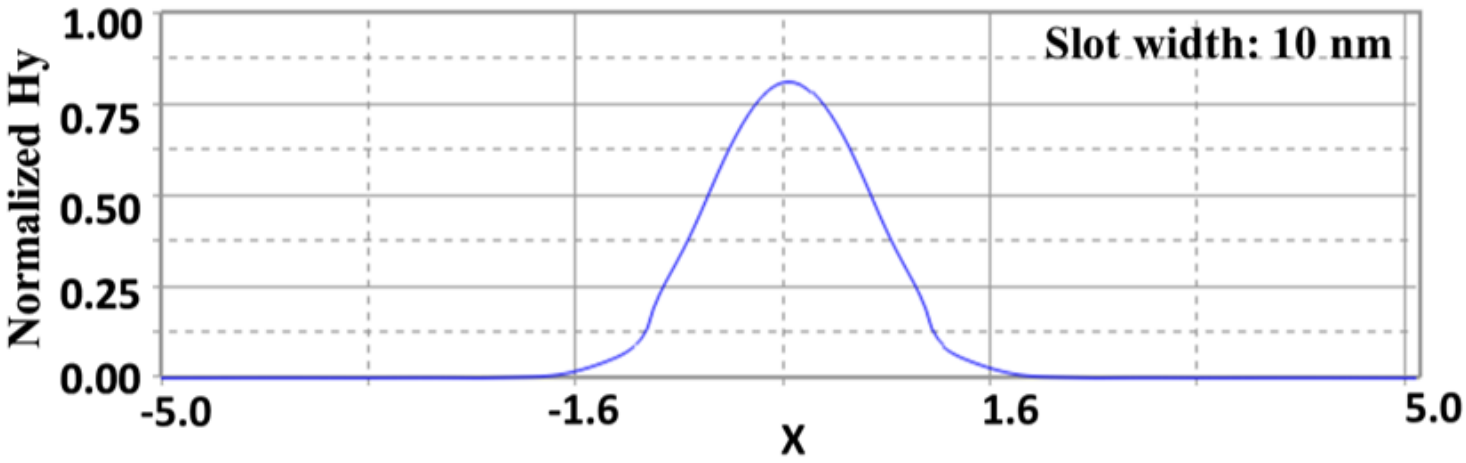

Figure 7

Optical power confinement profile in the core for the single vertical slot grating width of 10 nm.

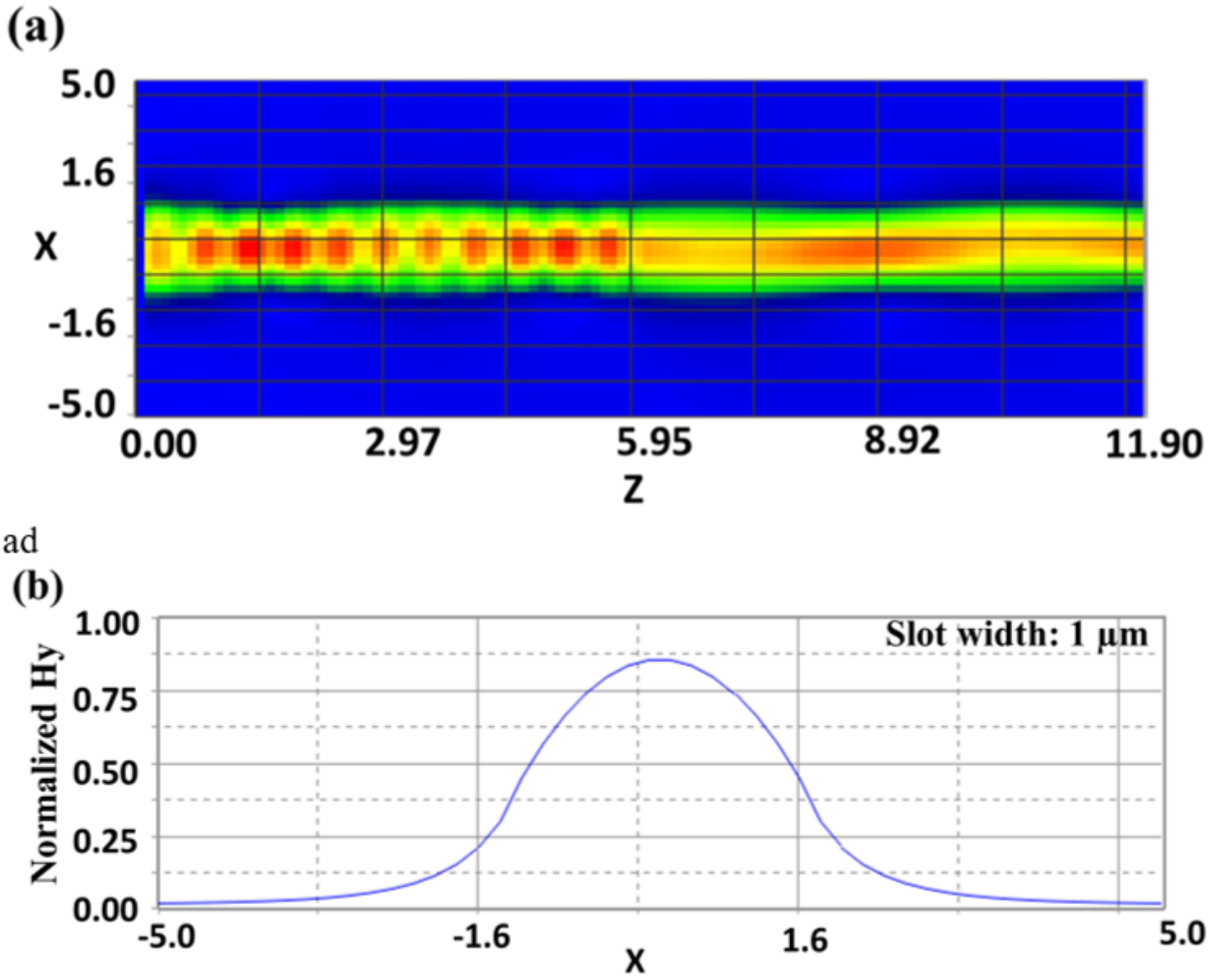

Figure 8

Analysis of plus shaped grating structure: (a) optical field propagation, and (b) optical field confinement within core.

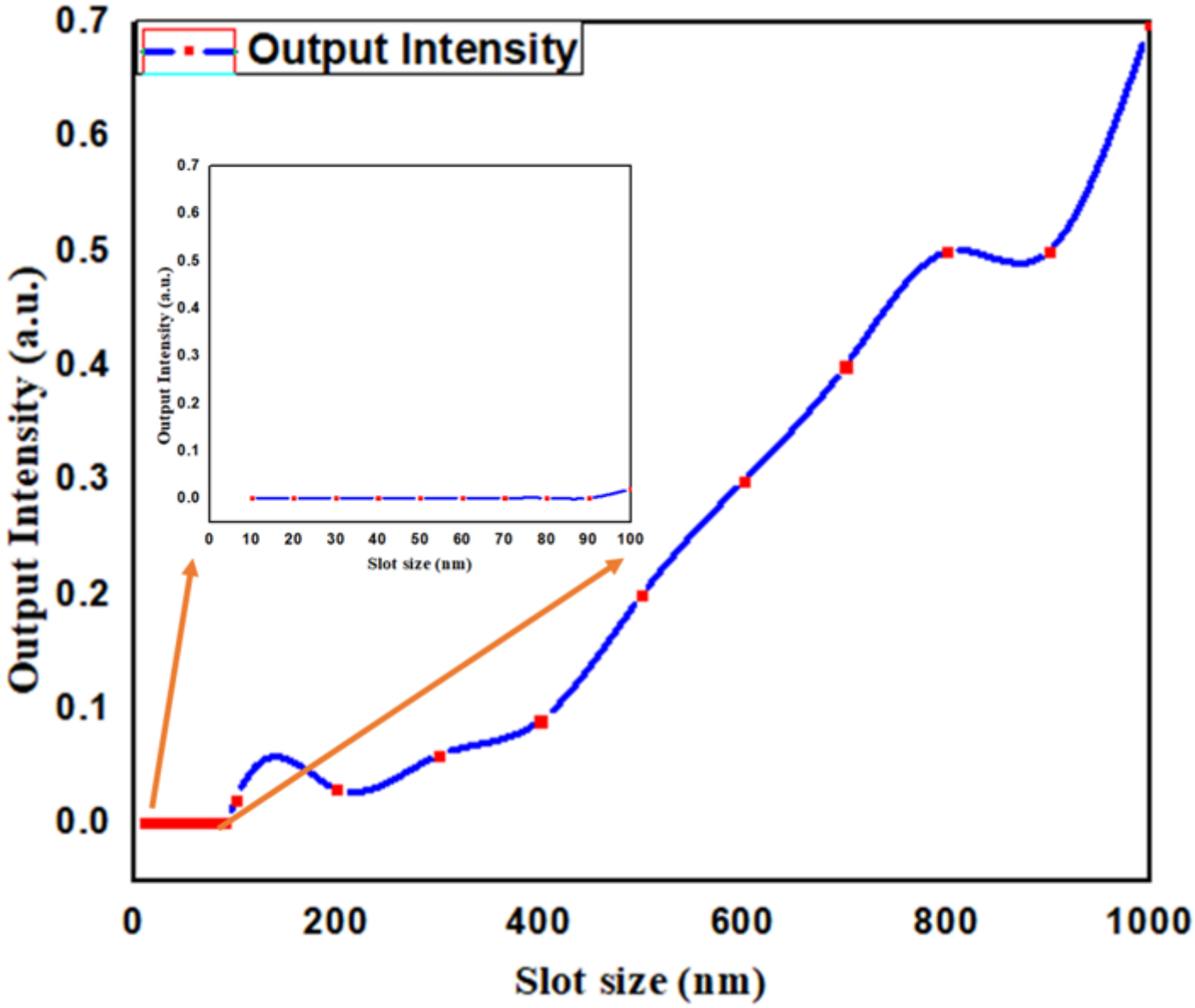

Figure 9

Plot output power transmission for different slot size of plus shaped grating.

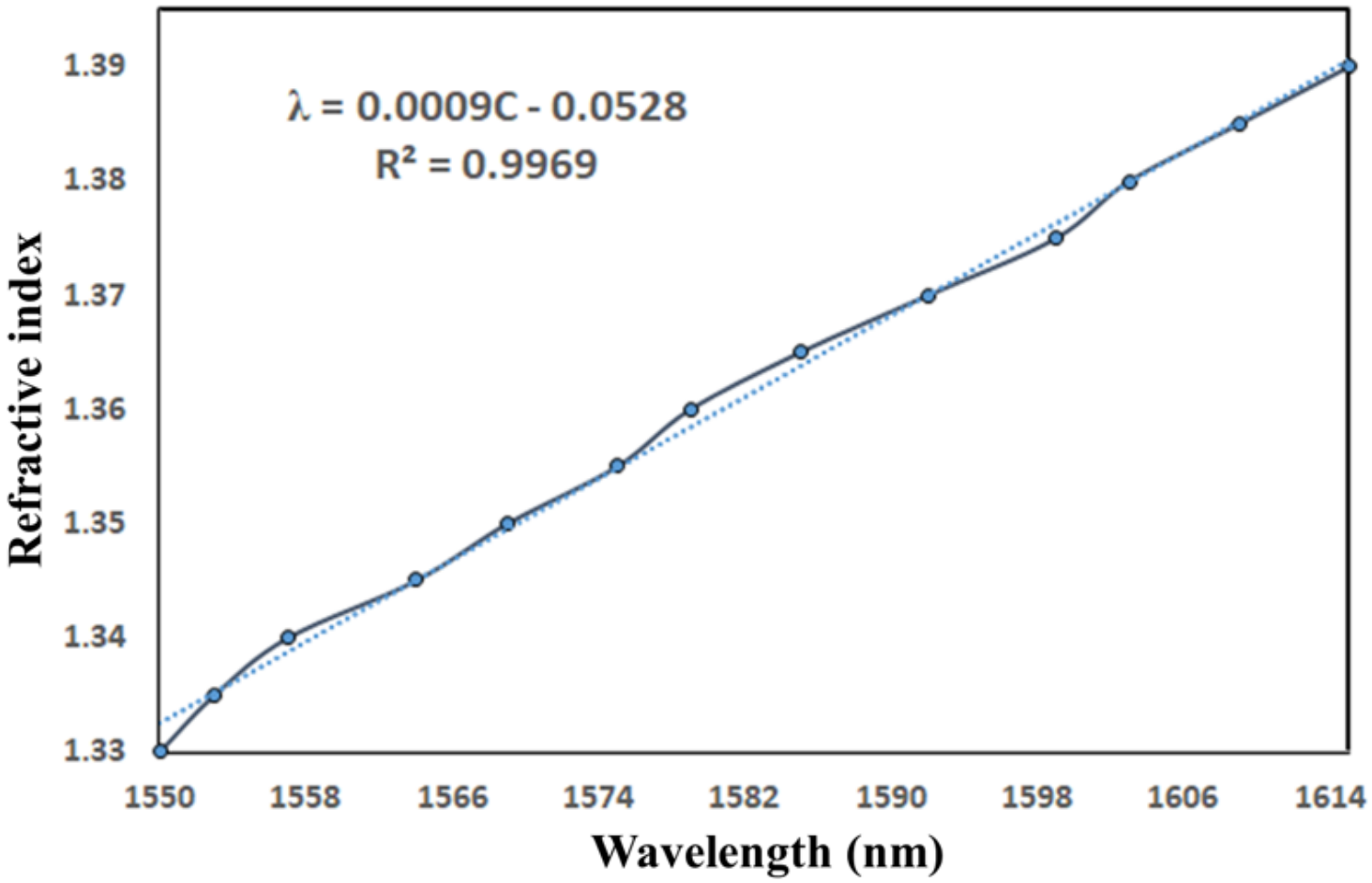

Figure 10

Autocorrelation curve of plus shaped grating structure.